Journal of Electronic Materials (2023) 52:1865–1874
https://doi.org/10.1007/s11664-022-10017-x

ORIGINAL RESEARCH ARTICLE

Improved Heat Resistance and Electrical Properties of Epoxy Resins by Introduction of Bismaleimide

Xubin Wang[1,2] · Tiandong Zhang[1,2] · Changhai Zhang[1,2] · Zhonghua Li[1,2] · Qingguo Chi[1,2]

Received: 8 July 2022 / Accepted: 3 October 2022 / Published online: 22 December 2022
© The Minerals, Metals & Materials Society 2022

Abstract

With the development of semiconductor power devices, packaging materials with excellent heat resistance and insulation properties are increasingly required. In this work, the heat resistance and electrical properties of epoxy resins (EP) are improved by introducing bismaleimide (BMI) with both imide ring and benzene ring structures. The results show that the introduction of BMI can increase the glass transition temperature (T_g) of the EP. The electrical conductivity and DC breakdown of BMI/EP are systematically investigated, and the results show that the electrical conductivity decreased and the DC breakdown field strength increased. The dielectric–temperature spectrum demonstrates that both the dielectric constant and dielectric loss decreased from room temperature to 150°C. In summary, the introduction of BMI improves the heat resistance and insulation properties of the BMI/EP, which shows good potential for use as high-temperature electronic packaging material.

Keywords Epoxy resins · heat resistance · electrical properties · electronic packaging

Introduction

Epoxy resin (EP), as one of most important insulation materials, is widely used in electrical and electronic equipment due to its insulation properties, chemical stability, strong adhesion, and low shrinkage.[1–4] However, the heat resistance of the common epoxy resin anhydride curing system (< 200°C) is too low to satisfy the needs of electronic packaging insulation materials.[5] For example, the third-generation SiC semiconductor power controller can operate normally at 600°C, which is much higher than the operating temperatures of first- and second-generation semiconductor power controllers.[6] However, the common EP cannot work at a temperature higher than 200°C. Besides, aerospace encapsulation materials need to withstand a temperature up to 220°C.[7] Therefore, it is essential to find an effective way to improve the heat resistance and electrical properties of EP for electronic packaging application.

It has been reported that the addition of inorganic fillers such as silica, alumina, and boron nitride can significantly improve the glass transition temperature (T_g) of EP-based composites,[8–10]; for example, Hu et al.[9] reported that the T_g increased from 136.7°C to 149.7°C when 40 vol.% Al_2O_3 was incorporated with neat epoxy. However, it usually requires a high content of inorganic fillers, and the aggregation of inorganic fillers and poor compatibility between organic and inorganic components are still the main bottlenecks in the preparation of composites. Researchers have used silicones or silane coupling agents to modify the surface of inorganic fillers and to improve the interfacial compatibility and dispersion of inorganic fillers and EP matrix.[11,12] However, the T_g improves just in a limited range due to the weak influence of inorganic fillers on the molecular structure–temperature stability. Another effective method is to increase the rigidity of the molecular chain by introducing benzene, naphthalene, an anthracene ring, biomass groups, etc.[13–17] For example, Qi et al.[13] reported that composites prepared by compounding an aromatic N-heterocyclic derived from biomass with epoxy resins showed an increase in glass transition temperature from

✉ Changhai Zhang
chzhang@hrbust.edu.cn

[1] Key Laboratory of Engineering Dielectrics and its Application, Ministry of Education, Harbin University of Science and Technology, Harbin 150080, People's Republic of China

[2] School of Electrical and Electronic Engineering, Harbin University of Science and Technology, Harbin 150080, People's Republic of China

173°C to 187°C, which not only can effectively improve the heat resistance of EP, but also can enhance flame retardant properties, toughness, etc. However, studies on electrical insulation properties are lacking.

Bismaleimide (BMI) has imide ring and benzene ring structures, with a T_g above 250°C; however, it can only be dissolved in organic solvents with strong polarity and high toxicity due to its high melting temperature and poor solubility. Interestingly, BMI can be completely melted and dispersed in EP after high-temperature heating. Therefore, BMI is chosen as a modification and is mixed with EP at a certain ratio to improve the heat resistance and electrical properties. The results show that the T_g and electrical insulation properties of composites are enhanced.

Experimental Section

Raw Materials

Epoxy resins were purchased from Shanghai Huayi Resin Co., Ltd., and the model number was AG-70. The curing agent was methyl hexahydrophthalic anhydride (MTHHPA), purchased from Changzhou Runxiang Electronic Materials. The mass ratio of EP to MTHHPA was 1:1.25. Bismaleimide was purchased from Beijing Innochem Science and Technology Co., Ltd. All chemical reagents were used directly without further purification.

Preparation of BMI/EP

The preparation process of the composites was as follows. Firstly, EP was weighed into a beaker, and then BMI was weighed and added according to 5 phr, 10 phr, 15 phr, and 20 phr of EP (abbreviated as 5 BMI/EP, 10 BMI/EP, 15 BMI/EP, and 20 BMI/EP, respectively), followed by stirring at 150°C for 2 h with a mechanical stirrer to fully dissolve BMI. After BMI was dissolved and dispersed evenly, the beaker was taken off and cooled to room temperature. Secondly, MTHHPA was added, and then the beaker was put into a vacuum oven and stirred for 0.5 h. Finally, the beaker was taken out, and the composites were pushed into the preheated mold with an injector and cured with a flat vulcanizer. The curing process was carried out at 140°C/2 h + 180°C/2 h.

Structure Characterization

The curing behaviors were analyzed via a Mettler differential scanning calorimeter. The test conditions were as follows: the uncured resin (range of 5–10 mg) was placed in an aluminum crucible and heated from 25°C to 270°C at rates of 5°C/min, 10°C/min, 15°C/min, and 20°C/min in a high-purity nitrogen atmosphere. Glass transition temperature tests were also performed on the cured EP.

Fourier transforms infrared (FTIR) spectroscopy (JASCO 6100) was used to analyze the molecular structure and chemical bonds of cured BMI/EP composites with different content.

The physical phase analysis of the composites was carried out using an x-ray diffractometer (XRD; PANalytical Corporation Empyrean).

Dynamic mechanical analysis (DMA) was performed on a TA Instruments Q800 dynamic mechanical analyzer in air. The sample with the dimension of $6 \times 1 \times 0.3$ cm^3 was tested at a heating rate of 3°C/min and a constant frequency of 1 Hz. The temperature range was from 30°C to 270°C.

The conductivity of the composites was tested at different temperatures with different field strengths using a laboratory-built three-electrode system, where the diameter of the test electrode was 50 mm, the protective electrode was a circle with an inner diameter of 54 mm and an outer diameter of 74 mm, and the diameter of the high-voltage electrode was 76 mm.

A direct-current (DC) electrical breakdown test system was used to test the breakdown field strength of the composites at different temperatures. The ramp speed of the applied voltage was 0.3 kV/s.

The variation of dielectric properties of the samples with temperature and frequency were measured using a broadband dielectric spectral instrument (Novocontrol Alpha-A).

Results and Discussion

Figure 1a and b shows the main chemical reaction process of EP and anhydride curing agent. Firstly, the hydroxyl group in EP reacts with anhydride and generates the ester group and carboxyl groups. Secondly, the formed carboxyl group rapidly reacts with the epoxy group rapidly to form another ester group and hydroxyl group, and then the hydroxyl group reacts with the epoxy group to form an ether bond. Figure 1c, d, and e shows the molecular structural formulae of AG-70 EP, MTHHPA, and BMI, respectively.

It is well known that the curing temperature has a deep impact on the curing process.[18] If the curing temperature is too low, the EP curing would be slow, and only the surface layer is cured, resulting in insufficient internal curing. If the curing temperature selection is too high, it causes explosive aggregation, leading to large internal stress. In order to select the optimal curing temperature, the non-isothermal differential scanning calorimetry (DSC) curve extrapolation method is used to determine the curing process of EP. As shown in Fig. 2a, the DSC curves with the different heating rates show one curing exothermic peak, meaning that only one

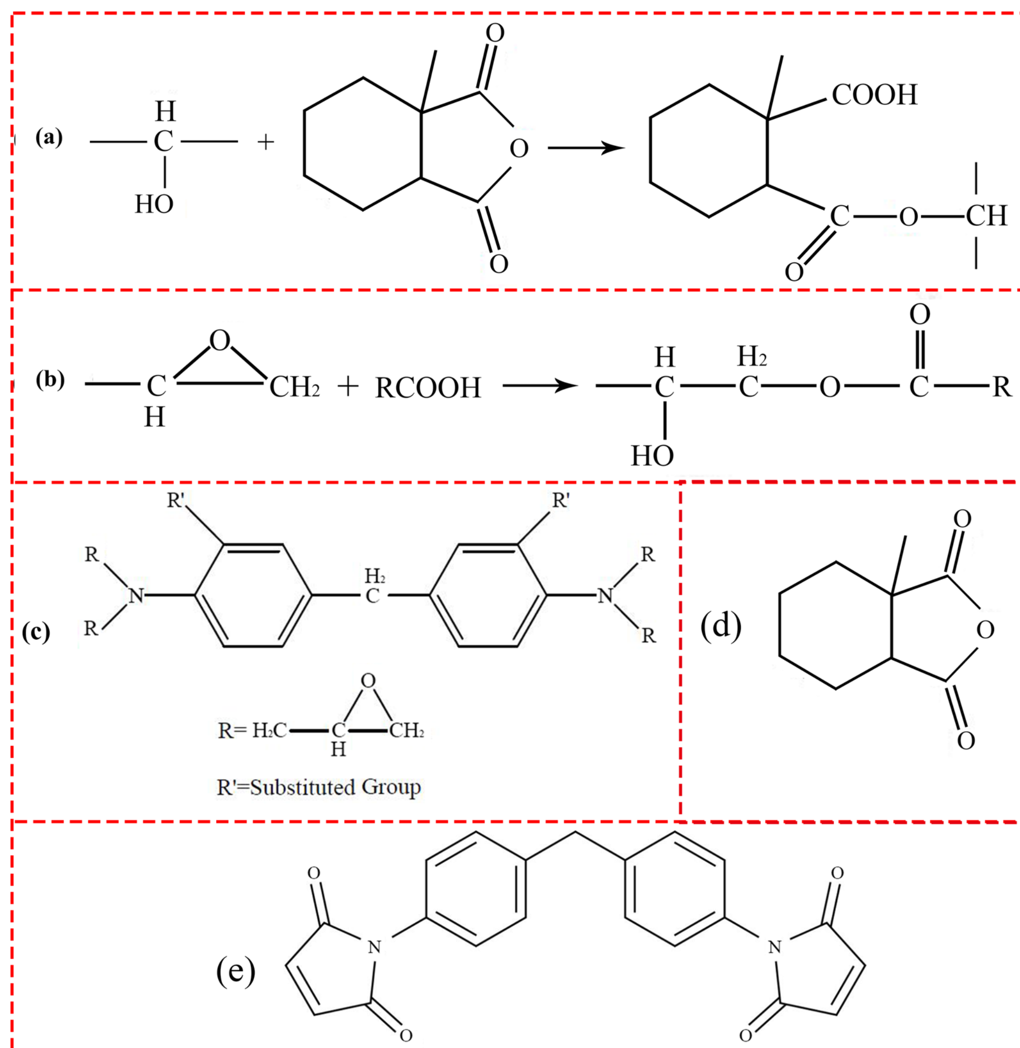

Fig. 1 (a, b) The main process of the curing reaction of epoxy resins and acid anhydride curing agent, (c) the structural formula of AG-70 epoxy resins, (d) methyl hexahydrophthalic anhydride curing agent, and (e) bismaleimide.

curing reaction in the system, and no other reactions occur. With the increase in heating rate β, the starting temperature (T_i), peak temperature (T_p), and termination temperature (T_f) of the curing reaction move to high temperature, the reaction heat hysteresis phenomenon occurs in the system, and the exothermic rate and heat release of curing reaction are increased. In the actual curing process, a gradient temperature rise is usually used. From the extrapolation method, the relationship between the values of T_i, T_p, and T_f and heating rate are fit linearly. The intercept with the T axis in the T–β fitting line corresponds to the heating rate of 0, which can be used as the curing temperature for the gradient temperature rising. Table I shows the characteristic parameters of DSC at different heating rates. Figure 2b shows the results of a linear fit of temperature versus heating rate. The theoretical cure onset temperature, i.e., gel temperature, is 66°C, the theoretical peak cure temperature is 139°C, and the theoretical cure termination temperature, i.e., post-treatment temperature, is 184°C. According to the abovementioned results, the curing temperature in this study is determined as 140°C/2 h and 180°C/2 h.

Kissinger's method is based on the relationship between the heating rate and the peak temperature of the curing reaction to calculate the curing kinetic parameters.[19] The method is not limited by the mechanism of the curing reaction system, so the method is widely used in the analysis of curing reaction kinetics. The formula is as follows:

$$\ln\left(\beta/T_p^2\right) = \ln(AR/E) - E/\left(RT_p\right) \quad (1)$$

where β is the heating rate, T_p is the exothermic peak temperature, R is the ideal gas constant (8.314 J/mol·K), E is the activation energy, and A is the pre-exponential. According to the linear fitting of $\ln\left(\beta/T_p^2\right)$ to $1/T_p$ of the

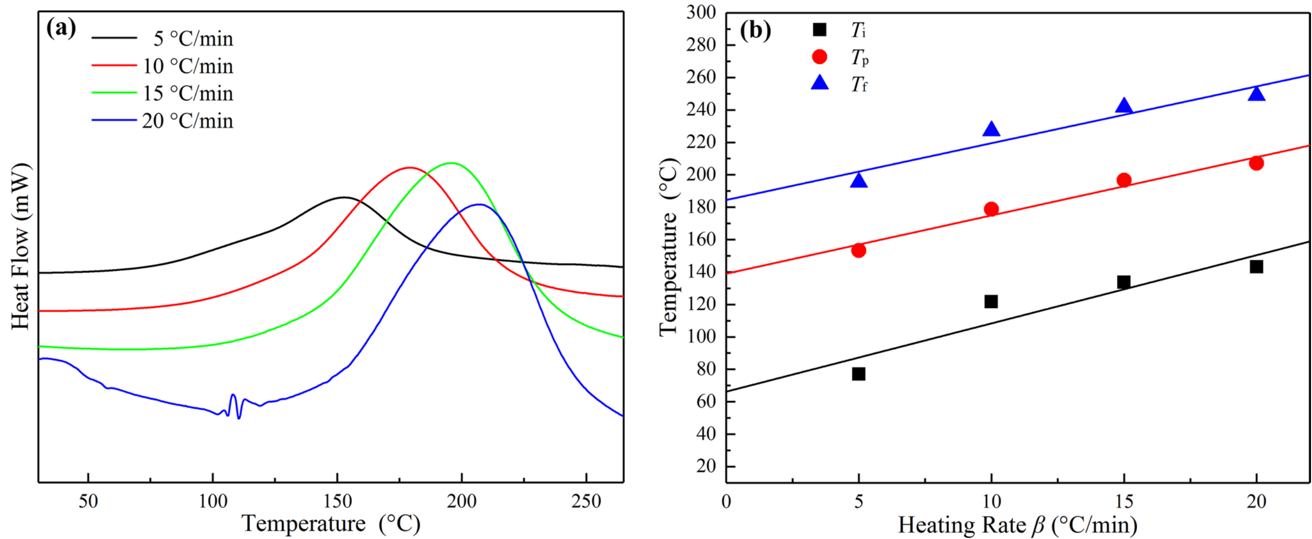

Fig. 2 (a) The DSC curves at different heating rates; (b) the linear fitting of temperature and heating rate T–β.

Table I The characteristic DSC parameters at different heating rates

Heating rate (°C/min)	T_i (°C)	T_p (°C)	T_f (°C)
5	76.99	153.2	195.35
10	121.7	178.79	227.08
15	133.58	196.57	241.76
20	143.19	207.17	248.86

composite system, the activation energy E of the curing reaction can be obtained from the slope of the straight line. From Fig. 3a, the slope of the linear fit is 4.30, the intercept is 0.43, and the reaction activation energy E is 35.75 kJ/mol by formula 1–1.

The Ozawa method can be used to directly obtain E and avoid the error caused by the different reaction mechanism functions.[19] The derived relational formula is

$$\ln \beta = -0.4567\frac{\Delta E}{RT} + \left[\ln \frac{A\Delta E}{T} - \ln F(X) - o2.315\right] \quad (2)$$

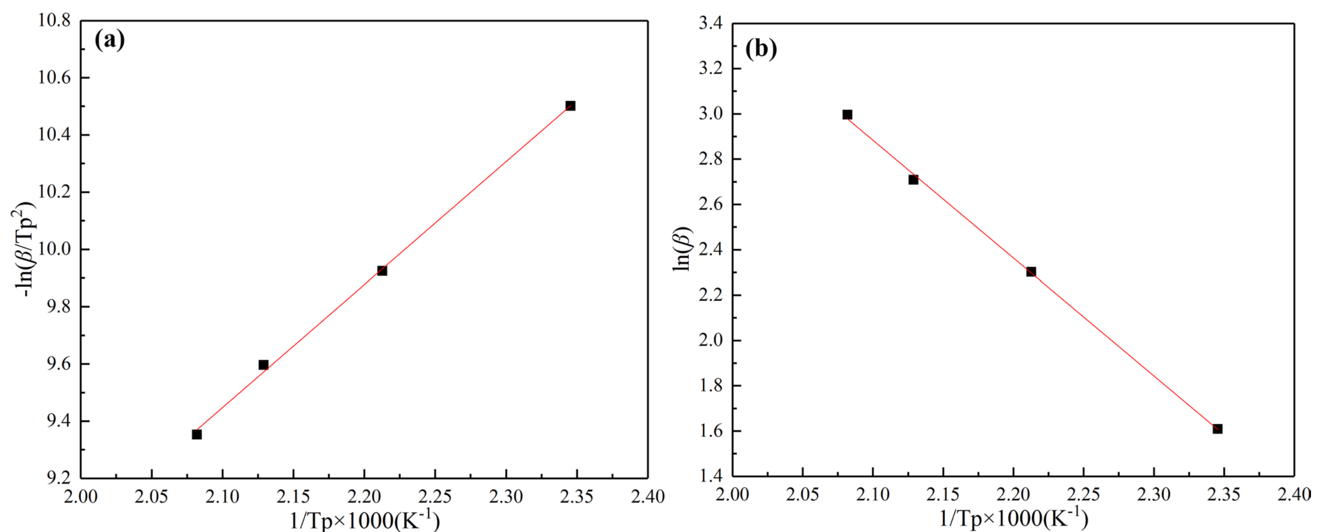

Fig. 3 (a) The relationship between $\ln\left(\beta/T_p^2\right)$ and $1/T_p \times 1000$ of the composites, (b) the relationship between $\ln(\beta)$ and $1/T_p \times 1000$ of composites.

where $F(X)$ is a function related to the conversion rate. Plotting $\ln\beta$ against $1/T_p$ at the same conversion rate, the slope is substituted into the following equation:

$$E = -\frac{R}{1.052}\frac{d\ln\beta}{d(1/T_p)} \quad (3)$$

From Fig. 3b, the slope and the intercept from the linear fitting are 5.20 and 13.8, respectively. The reaction activation energy E is 41.1 kJ/mol, which is slightly larger than that calculated by the Kissinger method. This is because the mathematical models established by the two calculation methods are different, and the reaction activation energy obtained is slightly different. However, the values of the reaction activation energy calculated by the two methods are close to each other, further indicating that the calculation results obtained are reliable.

The ratio of EP to MTHHPA is determined as 1:1.25 according to the formula of the amount of anhydride curing agent. Besides, the excess EP (1:0.75) or the excess MTHHPA (1:2) are also investigated for comparison. Figure 4a shows the infrared spectra of the EP and MTHHPA with different ratios, in which a wider transmission peak near 3550 cm^{-1} can be observed due to the remaining hydroxyl from EP when the ratio of EP/MTHHPA is 1:0.75. On the contrary, due to the excess of MTHHPA, when the ratio is 1:2, C=O of acid anhydride appears at 1860 cm^{-1}, and the remaining C=O of the anhydride disappears at a ratio of 1:1.25. Figure 4b shows the infrared spectroscopy of the BMI/EP. It can be seen that the peak of C=O transmission at 1860 cm^{-1} appears from BMI, and the peak intensity increases gradually with the increase in the BMI content. The AG-70 EP is tetrafunctional, and EP with multifunctional groups tends to suffer from incomplete curing due to steric hindrance and topological constraints.[7,20,21] Figure 4c shows the DSC results of the cured BMI/EP; only the weak peak of the heat absorption can be observed, and no other obvious exothermic peak exists at a temperature of 270°C, demonstrating that the curing conditions enable the curing reaction to complete well. Then it can be seen that the T_g of EP is about 200°C. After the introduction of BMI, the T_g of the composites cannot be obtained in the DSC curve, which is because the DSC is to determine the T_g by the change in specific heat capacity, and the DSC heat absorption signal of the composites is the same level before and after the T_g. Therefore, DMA, a method based on the change in modulus, is used to further measure the T_g values for the BMI/EP, where the modulus changes sharply at the critical temperature of T_g.[22] As shown in Fig. 4d, the energy storage modulus of 20 BMI/EP is about 3250 MPa at 30°C, which is 1.3 times that of pure EP (2500 MPa). T_g is determined by the peak temperature of tanδ as shown in Fig. 4e, which is 220°C and 243°C for pure EP and 20 BMI/EP, respectively. The increase in energy storage modulus and T_g is mainly attributed to the increase in stiffness due to the imide ring and benzene ring in BMI, indicating that the BMI/EP can be used as high heat resistance packaging materials, such as in the field of the aerospace ($T_g \geq 220$°C).[7] Figure 4f shows the XRD pattern of the BMI/EP; two characteristic peaks with approximately equal intensity at low angles indicate that AG-70 EP is an amorphous polymer. With the increase in BMI content, the relative intensity of the two characteristic diffraction peaks changes a lot; the increased diffraction peaks can be attributed to BMI. There are no other miscellaneous peaks, indicating that it is only a simple physical co-mixed and non-chemical reaction between EP and BMI.

In order to evaluate the insulation of the BMI/EP, the DC electrical conductivity and electrical breakdown strength were measured at room temperature (RT, 23°C ± 2°C) and 80°C as shown in Fig. 5. It can be seen that the conductivity gradually increases with the increase in the electric field in Fig. 5a. What is more obvious is that the conductivity decreases with the increase in BMI content, indicating that the insulation performance becomes more excellent by introduction of BMI. This may be due to the intertwining of the molecular chains of EP and BMI on the microscopic level, enabling the molecular chains to be tighter and the free travel of carriers to be shorter under the applied electric field, resulting in a decrease in conductivity at the macroscopic level. It was also reported that the C=O carbonyl polar groups from the BMI is beneficial to forming the deep trap energy levels and trapping the electric charge carrier.[23] The conductivity of the composites increases by 1–2 orders of magnitude at 80°C, as shown in Fig. 5b, but still maintains good insulation properties. Figure 5c and d shows the Weibull breakdown field strength at room temperature and 80°C, respectively. It can be seen that the breakdown field strength of pure EP is the lowest and increases gradually with the increase in BMI content. The variation law of the breakdown field strength at 80°C is similar to that of room temperature, but the overall breakdown field strength is lower than the room temperature, which can be perfectly corresponded to the DC conductivity. The Weibull parameters are shown in the Fig. 5c and d. The breakdown field strength is 232.7 kV/mm for EP and 257.2 kV/mm for 20 BMI/EP at room temperature and 186.3 kV/mm for EP and 218.5 kV/mm for 20 BMI/EP at 80°C.

Figure 6 shows the temperature dependence changes in the dielectric constant and dielectric loss for the BMI/EP. The dielectric constants of EP, 5 BMI/EP, and 10 BMI/EP decrease firstly and then increase with increasing temperature in the temperature range from room temperature to 150°C, and 15 BMI/EP and 20 BMI/EP show a monotonic increase, which is due to the increase in dipole polarization with increasing temperature. The change in dielectric constant is very small, e.g., 3.84 for EP at room temperature

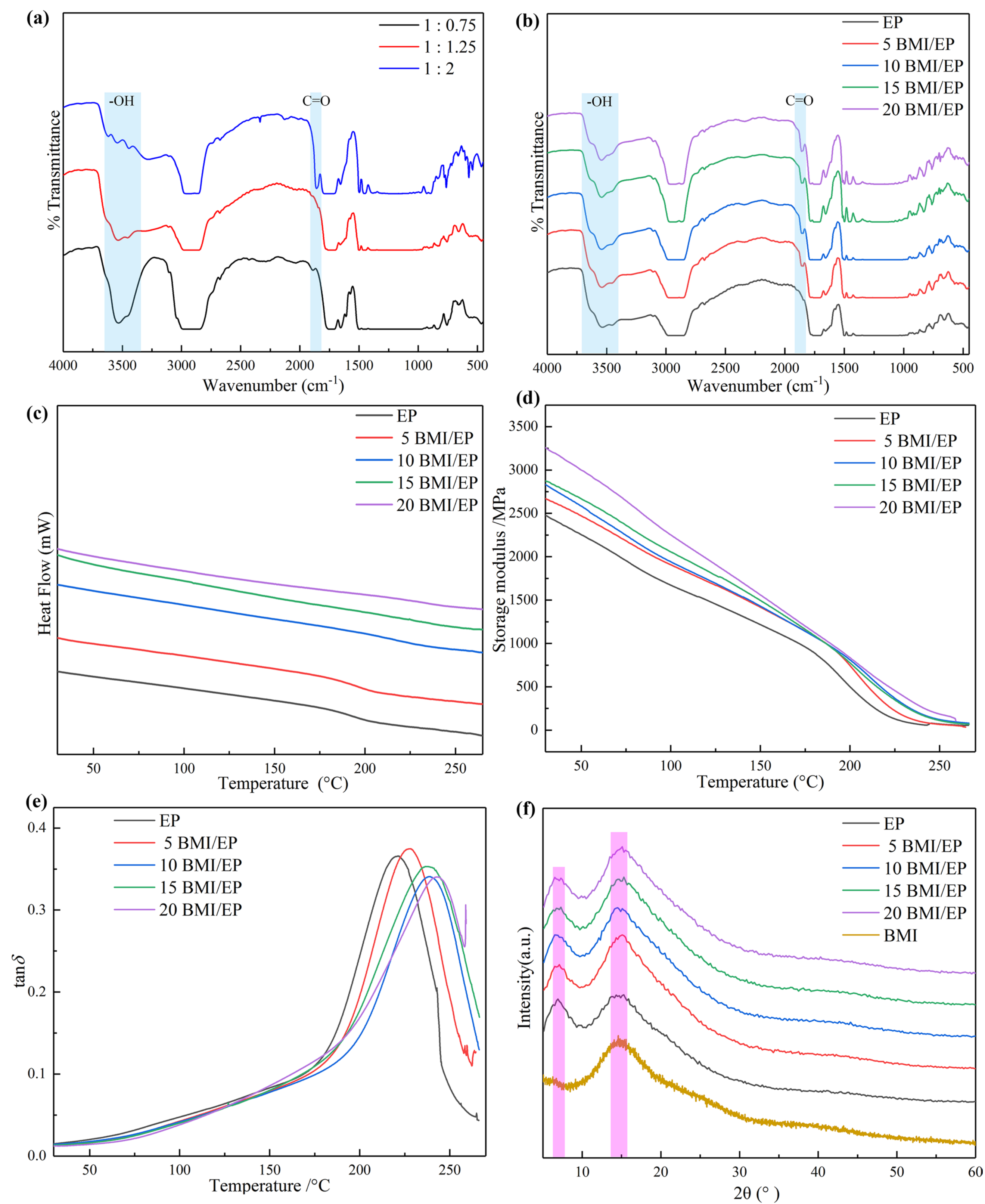

Fig. 4 (a) Infrared spectra of the EP cured with different ratios of curing agent, (b) infrared spectra of the BMI/EP, (c) DSC of the BMI/EP, (d) storage modulus and (e) tanδ of the BMI/EP, (f) XRD of the BMI/EP.

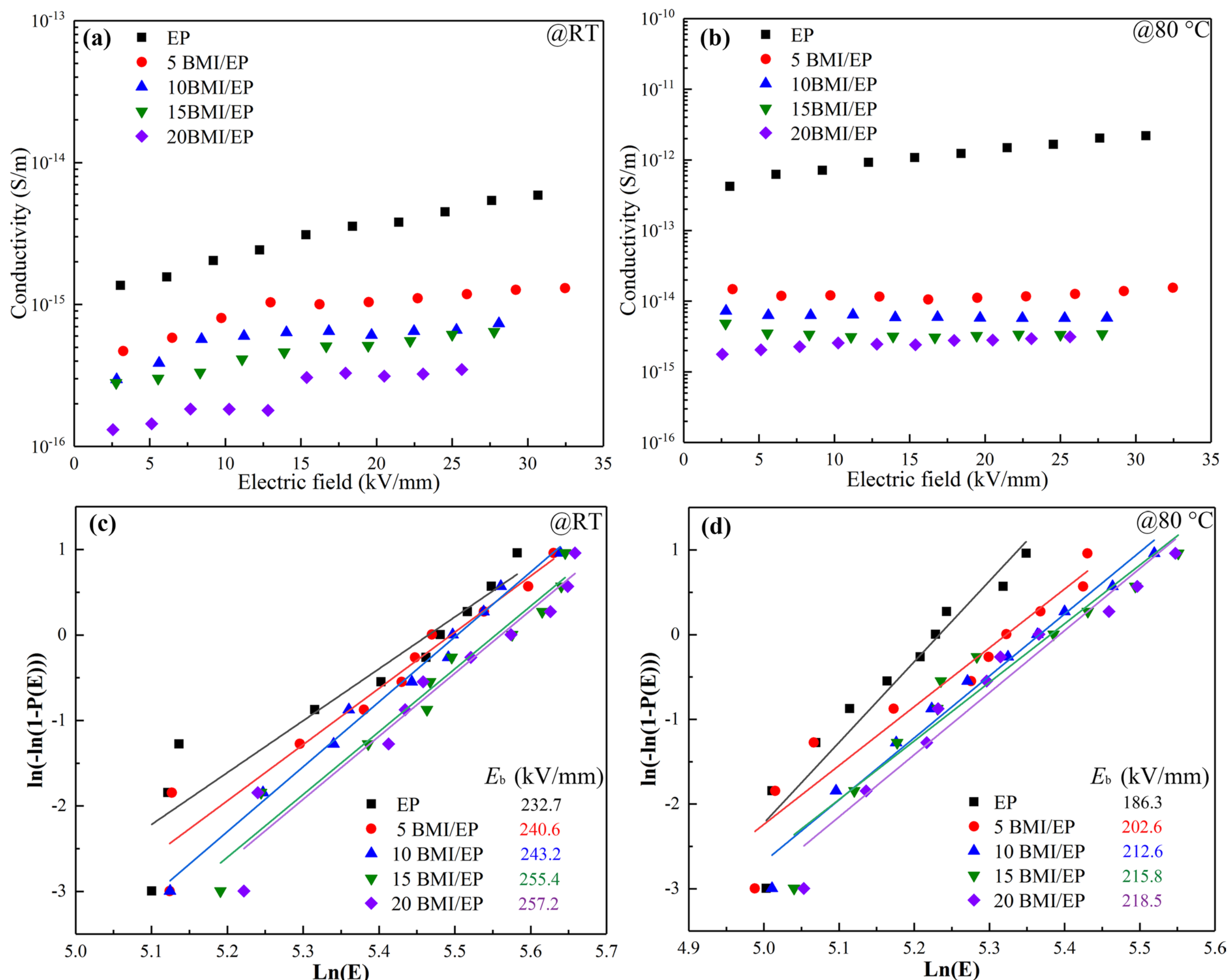

Fig. 5 DC conductivity of the BMI/EP at (a) room temperature and (b) at 80°C. Weibull DC breakdown field of the BMI/EP at (c) room temperature and (d) at 80°C.

and 3.99 at 150°C for 100 Hz, and 3.49 for 20 BMI/EP at room temperature and 3.73 at 150°C, probably because 150°C is far below its T_g and does not cause a large change in the dielectric constant of the material. As the frequency increases from 10^2 Hz to 10^6 Hz, the dielectric constant of the composite tends to decrease because the dipole steering polarization does not keep up with the change in the external electric field. The dielectric loss decreases with increasing temperature in the temperature range from room temperature to 150°C from 10^2 Hz to 10^4 Hz and then decreases from 10^5 Hz to 10^6 Hz. The relaxation polarization loss gradually decreases with increasing temperature, and the ionic conductivity loss starts to increase with a further increase in temperature. As the frequency increases, the loss also becomes progressively larger. However, it is lower than 0.02 in the frequency range of 10^2 Hz to 10^6 Hz.

Figure 7 shows the dielectric constant and dielectric loss of BMI/EP with different content at (a) RT, (b) 80°C, and (c) 150°C. It can be seen that the dielectric constant and dielectric loss of EP decrease with the increase in BMI content at the same temperature. This is because the increase in cross-link density and intermolecular tightness reduce the dipole moment of the chain segments. In addition, it is also due to the greater rigidity of the BMI molecular chains, whose dipole loss is smaller in a wide temperature range, so that the composites can have better dielectric properties.

Conclusion

In this work, the non-isothermal DSC curve extrapolation method was used to determine the curing process of EP. T_g of the BMI/EP was tested by DMA, and it was found that

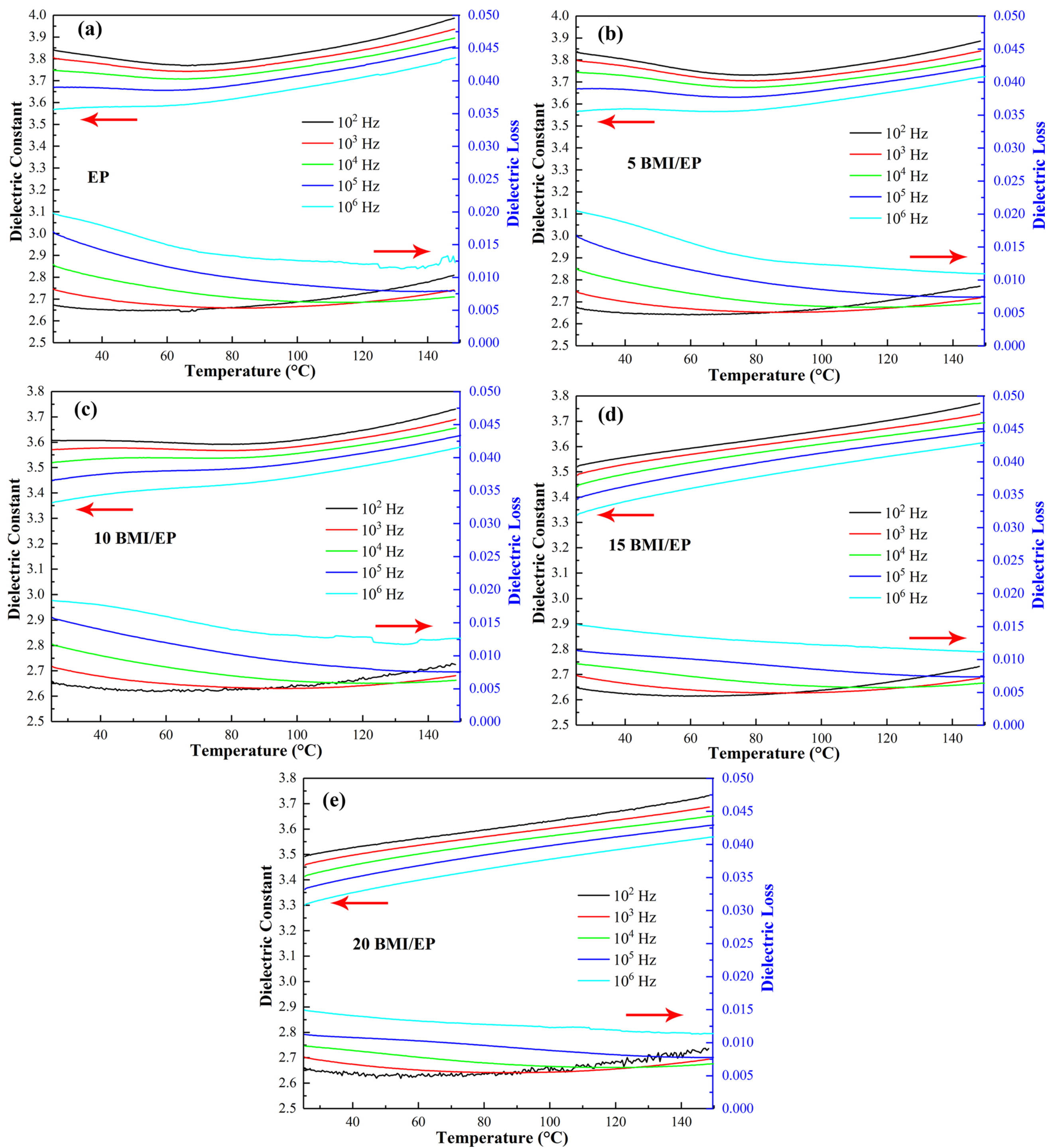

Fig. 6 Temperature-dependent changes in the dielectric constant and the dielectric loss for the BMI/EP, (a) EP, (b) 5 BMI/EP, (c) 10 BMI/EP, (d) 15 BMI/EP, (e) 20 BMI/EP.

the T_g of the BMI/EP gradually increased with the increase in BMI content. Through systematic investigation of the electrical conductivity and DC breakdown of BMI/EP, it was found that the electrical conductivity decreased and the DC breakdown field strength increased, indicating that the insulation properties of BMI/EP increased with the increase in BMI content. The introduction of BMI decreased the dielectric constant and dielectric loss of EP. In conclusion, the introduction of BMI can increase the T_g of EP, increase the electrical insulation properties, and reduce the dielectric

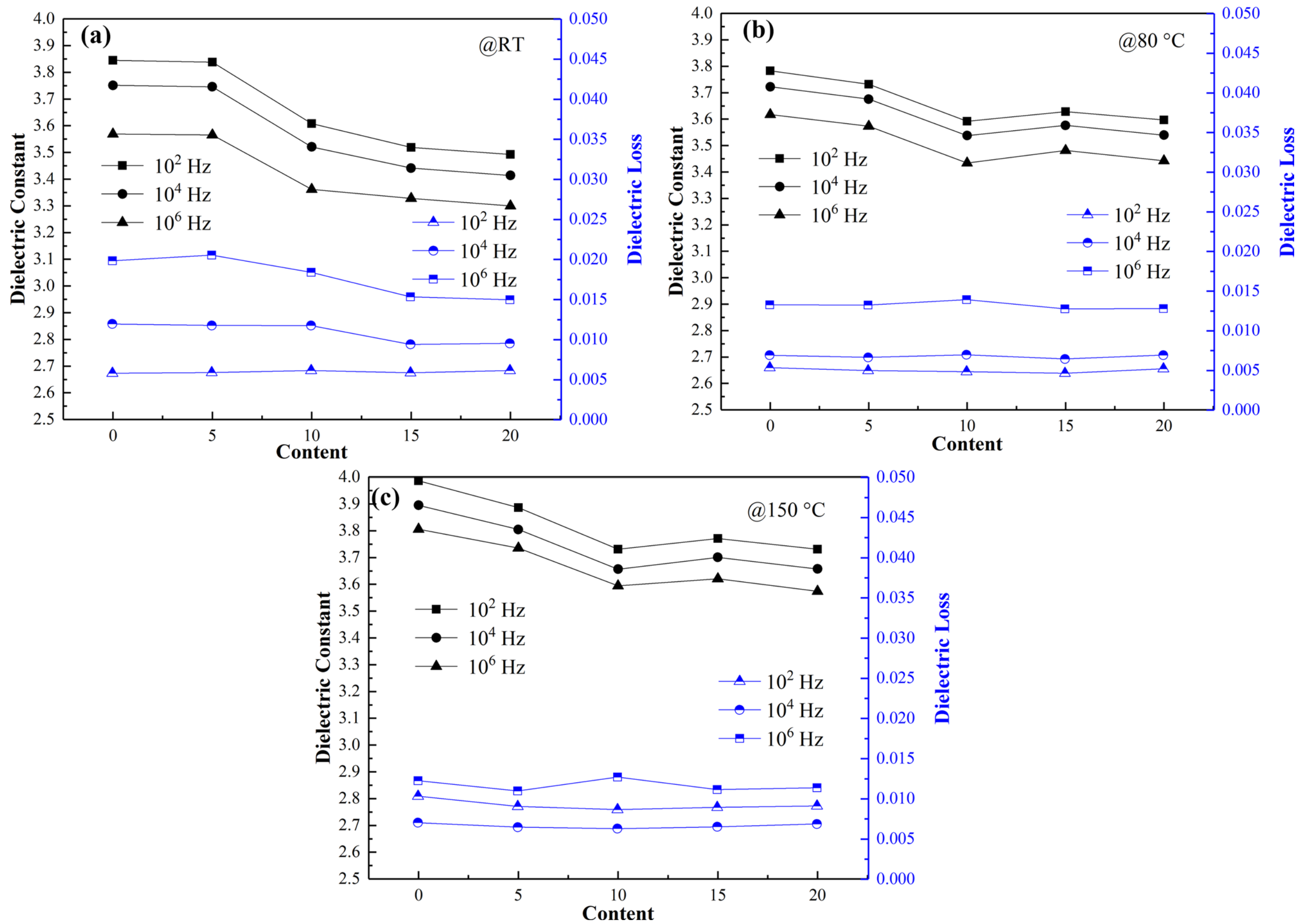

Fig. 7 Dielectric constant and dielectric loss of BMI/EP with different content at (a) RT, (b) 80°C, (c) 150°C.

constant and dielectric loss. This will be beneficial for the application of EP in high-temperature insulation packages.

Acknowledgments This study was funded by the National Natural Science Foundation of China (52007042), Natural Science Foundation of Heilongjiang Province of China (No. TD2019E002), and China Postdoctoral Science Foundation (No. 2021T14066).

Conflict of interest The authors declare that they have no conflict of interest.

References

1. F. Fang, S. Ran, Z. Fang, P. Song, and H. Wang, *Part B-Eng.* 165, 406 (2019).
2. R. Chen, K. Hu, H. Tang, J. Wang, F. Zhu, and H. Zhou, *Polym. Degrad. Stabil.* 166, 334 (2019).
3. Y. Xue, M. Shen, S. Zeng, W. Zhang, L. Hao, L. Yang, and P. Song, *Mater. Res. Express* 6, 125003 (2019).
4. L. Liu, Y. Xu, M. Xu, Z. Li, Y. Hu, and B. Li, *Compos. Part B Eng.* 167, 422 (2019).
5. K. Fu, Q. Xie, F. Lü, Q. Duan, X. Wang, Q. Zhu, and Z. Huang, *Polymers* 11, 975 (2019).
6. V. Abou Hamad, T. Abi Tannous, M. Soueidan, L. Gremillard, D. Fabregue, J. Penuelas, and Y. Zaatar, *Microelectron. Reliab.* 110, 113694 (2020).
7. T. Liu, L. Zhang, R. Chen, L. Wang, B. Han, Y. Meng, and X. Li, *Ind. Eng. Chem. Res.* 56, 7708 (2017).
8. S.K. Singh, A. Kumar, S. Singh, A. Kumar, and A. Jain, *Mater. Today Proc.* 38, 2861 (2021).
9. Y. Hu, C. Chen, Y. Wen, Z. Xue, X. Zhou, D. Shi, G. Hu, and X. Xie, *Compos. Sci. Technol.* 209, 108760 (2021).
10. X. Yang, Y. Guo, X. Luo, N. Zheng, T. Ma, J. Tan, C. Li, Q. Zhang, and J. Gu, *Compos. Sci. Technol.* 164, 59 (2018).
11. J. Li and S. Li, *Mater. Chem. Phys.* 274, 125151 (2021).
12. D. Yang, Y. Ni, X. Kong, D. Gao, Y. Wang, T. Hu, and L. Zhang, *Compos. Sci. Technol.* 177, 18 (2019).
13. Y. Qi, J. Wang, Y. Kou, H. Pang, S. Zhang, N. Li, C. Liu, Z. Weng, and X. Jian, *Nat. Commun.* 10, 1 (2019).
14. Y. Qi, Z. Weng, Y. Kou, H. Pang, S. Zhang, N. Li, C. Liu, Z. Weng, and X. Jian, *Chem. Eng. J.* 406, 126881 (2021).
15. F. Zhang, L. Zong, F. Bao, Z. Weng, C. Wang, J. Wang, and X. Jian, *Polym. Adv. Technol.* 31, 635 (2020).
16. F. Zhang, L. Zong, Z. Weng, F. Bao, N. Li, J. Wang, and X. Jian, *Compos. Part A Appl. Surf.* 131, 105772 (2020).
17. X. Dong, M. Zheng, B. Wan, X. Liu, H. Xu, and J. Zha, *Materials* 14, 6266 (2021).
18. H. Ma, X. Zhang, F. Ju, and S.B. Tsai, *Sci. Rep* 8, 1 (2018).
19. F. Boey and W. Qiang, *Polymer* 41, 2081 (2000).

20. K. Riad, R. Schmidt, A. Arnold, and R. Wuthrich, *Polymer* 104, 83 (2016).
21. K. Pingkarawat, C. Dell'Olio, R. Varley, and A.P. Mouritz, *Compos. Part A Appl. S.* 78, 201 (2015).
22. K. Smith, T. Lazzara, and R. Fernando, *J. Appl. Polym. Sci.* 138, 51221 (2021).
23. Y. Zhou, C. Yuan, S. Wang, Y. Zhu, S. Cheng, X. Yang, Y. Yang, J. Hu, J. He, and Q. Li, *Energy Storage Mater.* 28, 255 (2020).

Publisher's Note Springer Nature remains neutral with regard to jurisdictional claims in published maps and institutional affiliations.

Springer Nature or its licensor (e.g. a society or other partner) holds exclusive rights to this article under a publishing agreement with the author(s) or other rightsholder(s); author self-archiving of the accepted manuscript version of this article is solely governed by the terms of such publishing agreement and applicable law.